MEDICAL SCIENCE MONITOR

CLINICAL RESEARCH

e-ISSN 1643-3750
© Med Sci Monit, 2015; 21: 376-382
DOI: 10.12659/MSM.892534

Received: 2014.09.20
Accepted: 2014.12.28
Published: 2015.02.01

Parameters of Dynamic Contrast-Enhanced MRI as Imaging Markers for Angiogenesis and Proliferation in Human Breast Cancer

Authors' Contribution:
Study Design A
Data Collection B
Statistical Analysis C
Data Interpretation D
Manuscript Preparation E
Literature Search F
Funds Collection G

AE 1 Lin Li
B 2 Kai Wang
C 2 Xilin Sun
D 2 Kezheng Wang
CF 2 Yingying Sun
D 1 Guangfeng Zhang
AF 1,2 Baozhong Shen

1 Department of Radiology, Fourth Hospital of Harbin Medical University, Harbin, Heilongjiang, P.R. China
2 Molecular Imaging Center, Harbin Medical University, Harbin, Heilongjiang, P.R. China

Corresponding Author: Baozhong Shen, e-mail: shenbzh@vip.sina.com
Source of support: This work was supported, in part, by the National Natural Science Foundation of China (81130028, 31210103913), the Key Grant Project of Heilongjiang Province (GA12C302), the Ph.D. Programs Foundation of Ministry of Education of China (201123071100203), and the Key Laboratory of Molecular Imaging Foundation (College of Heilongjiang Province)

Background: Breast cancer is the most common malignancy and the leading cause of cancer death in women worldwide; however, early diagnosis has been difficult due to its complex pathological structure. This study evaluated the value of morphological examination in conjunction with dynamic contrast-enhanced MRI (DCE-MRI) for more precise diagnosis of breast cancer, as well as their correlation with angiogenesis and proliferation biomarkers.

Material/Methods: DCE-MRI parameters (including K^{trans}: volume transfer coefficient reflecting vascular permeability, K_{ep}: flux rate constant, V_e: extracellular volume ratio reflecting vascular permeability, and ADC: apparent diffusion coefficient) were obtained from 124 patients with breast cancer (124 lesions). Microvessel density (MVD) was evaluated by the immunohistochemical analysis of tumor vessels for CD31 and CD105 expression. The proliferation was assessed by analyzing Ki67.

Results: K^{trans} values were in the order of: malignant lesions > benign lesions > normal glands. Similar results were observed for K_{ep}. The opposite changes were seen with V_e. K^{trans} and K_{ep} values were significantly higher in invasive ductal carcinoma (IDC) and ductal carcinoma *in situ* (DCIS) than in mammary ductal dysplasia (MDD; ANOVA followed by Dunnett's test). In sharp contrast, ADC values were lower in IDC and DCIS than in MDD, and V_e was not significantly different among the three groups. The data from MIP (maximum intensity projection) showed that benign breast lesions had no or only one blood vessel, whereas malignant lesions had two or more blood vessels. In addition, expression of CD105 and Ki67, the commonly recognized markers for angiogenesis and proliferation, respectively, were closely correlated with MRI parameters as revealed by Pearson analysis.

Conclusions: Determination of K^{trans}, K_{ep} and ADC values permits estimation of tumor angiogenesis and proliferation in breast cancer and DCE-MRI parameters can be used as imaging biomarkers to predict patient prognosis and the biologic aggressiveness of the tumor.

MeSH Keywords: Cell Proliferation • Magnetic Resonance Imaging • Neovascularization, Pathologic

Full-text PDF: http://www.medscimonit.com/abstract/index/idArt/892534

2881 5 1 24

Indexed in: [Current Contents/Clinical Medicine] [SCI Expanded] [ISI Alerting System] [ISI Journals Master List] [Index Medicus/MEDLINE] [EMBASE/Excerpta Medica] [Chemical Abstracts/CAS] [Index Copernicus]

Background

Tumor progression and metastasis are angiogenesis-dependent and quantification of tumor angiogenesis has prognostic value in breast cancer. Magnetic resonance imaging (MRI) is considered a highly sensitive, noninvasive technique for the detection of breast cancer [1]. Of all MRI techniques used for assessment of breast cancer, dynamic contrast enhanced MRI (DCE-MRI) is the most established and widely used. DCE-MRI has been reported to have sensitivity of 88–100% and specificity of 68–96% for cancer detection [2,3]. Recently, MRI has been used to analyze combined morphologic characteristics and kinetic enhancement patterns of breast lesions, and integration of these parameters offers an enhanced predictive power [4,5].

Angiogenesis is the term describing the complex process leading to the formation of new blood vessels from the preexisting vascular network [6]. The growth, invasion, and metastasis of cancers depend on angiogenesis, and quantification of tumor microvasculature is thus considered an approach for anti-angiogenic therapy of cancers [7]. The association of CD105 with angiogenesis was initially identified by Wang et al. [8], who observed that monoclonal antibodies to CD105 reacted strongly with the endothelium in various tumor tissues but only weakly in normal tissues [9]. On the other hand, unlimited proliferation is one of the most important characteristics of cancer. Studies revealed that Ki67 is highly expressed in proliferative cells in many kinds of cancers, but rarely in normal cells [10].

In this study, we investigated that there is any correlation between angiogenesis and proliferation of tumors and DCM-MRI parameters including K^{trans} (volume transfer coefficient reflecting vascular permeability), K_{ep} (flux rate constant), V_e (extracellular volume ratio reflecting vascular permeability) and ADC (apparent diffusion coefficient) so as to assess the diagnostic value of DCE-MRI for breast lesions. To gain insight into the mechanisms associated with tumor angiogenesis, we also investigated the relationship between the DCE-MRI parameters and expression levels of vascular markers CD31, CD105 and Ki67.

Material and Methods

Subjects

The study enrolled 124 patients with breast carcinoma ranging from 23 to 76 years old (mean ±SD=49.1±11.9 years) under the procedures approved by the Ethnic Committee for Use of Human Samples of Harbin Medical University. These patients all underwent surgery (lumpectomy or mastectomy) from September 2011 to October 2013, and they did not receive chemotherapy or hormone therapy prior to surgery. The inclusion criteria were: (1) Gender: women; (2) Age: 18 years or older; and (3) Therapy: not receiving chemotherapy or hormone therapy prior to surgery. And the exclusion criteria were: (1) currently lactating and (2) currently being pregnant. Conventional MRI scan, DWI and DCE-MRI dynamic contrast-enhanced scan were performed on the patients, within two weeks post surgery. All measurements were examined by three senior pathologists experienced in breast carcinoma diagnosis and screening from the First, the Third and the Fourth Hospitals affiliated to the Harbin Medical University, respectively, and they worked independently in a double-blinded manner.

MRI study protocol

MRI was performed using the 3.0 T Achieva (Philips, Netherland). Patients were scanned in prone position, eupnea, with the bilateral breast naturally suspended in the breast coil. Conventional sequences and scan parameters were: (1) T2-SPAIR fat suppression sequences, TR60, ms; TE, 4000 ms; FOV, 24×34×15 cm; thickness, 3 mm; gap, 0 mm; matrix, 300×325; NSA, 2; (2) Coronal 3De-THRIVE, TR, 3 ms; TE, 1.4 ms; FOV, 37.5×40×7 cm; thickness, 4 mm; gap, 0 mm; matrix, 512×512; NSA, 2; (3) The diffusion-weighted images (DWI) were acquired with the following parameters: TR, 2900 ms; TE, 64 ms; FOV, 35×24×15 cm; thickness, 3 mm; gap, 0 mm; matrix, 256×256; NSA; and (4) Dynamic contrast-enhanced axial scans using 3D fast low-angle shot dynamic imaging sequences (FLASH-3D). Scan parameters were as follows: TR, 4.5 ms; TE, 2.2 ms; FOV, 25×34×9 cm; matrix, 256×256; scan layers, 75. For dynamic MRI, gadopentetate dimeglumine (Gd-DTPA) was intravenously injection at 2 mL/s, 0.15 mmol/kg using a power injector (Sonic Shot 50; Nemoto Kyorindo, Tokyo, Japan), followed by 20 mL saline flush. After scanning, the images were transmitted to strengthen the image and make maximum signal projection (maximum intensity projection, MIP) images.

Interpretation of MRI Measurements

DCE-MRI parameters (including K^{trans}: volume transfer coefficient reflecting vascular permeability, K_{ep}: flux rate constant, V_e: extracellular volume ratio reflecting vascular permeability, and ADC: apparent diffusion coefficient) were measured.

Post-processing of the measurements was performed off-line on a Pentium IV personal computer with Philips Achieva. Breast MRI was retrospectively reviewed by two experienced radiologists. The breast MRI was analyzed according to the criteria set by the American College of Radiology Breast Imaging Reporting and Data System, including tumor shape (round, oval, lobular, or irregular), margin (smooth, irregular, or spiculated), and internal enhancement (homogeneous, heterogeneous, rim enhancement, dark internal septa, enhancing internal septa, or central enhancement). In addition, we analyzed

Indexed in: [Current Contents/Clinical Medicine] [SCI Expanded] [ISI Alerting System] [ISI Journals Master List] [Index Medicus/MEDLINE] [EMBASE/Excerpta Medica] [Chemical Abstracts/CAS] [Index Copernicus]

and calculated tumor size, pattern of time–signal intensity (TSI) curve, and the ADC value.

For the signal-intensity analysis, the areas with the highest visual enhancement were chosen as regions of interest (ROIs) for evaluating the enhancement pattern and TSI curves were constructed. Kinetic analysis was performed based on the Breast Imaging Reporting and Data System MRI guidelines. Depend on the images obtained during the last four phases of contrast-enhanced dynamic imaging, TSI curve patterns were classified into three types: (1) the persistent pattern, with a continuous increase in the signal intensity over time; (2) the plateau pattern, in which the signal intensity does not change after its initial increase; and (3) the washout pattern, with an initial increase and reaching the highest point, then followed by a decrease of the signal intensity.

ROIs were used for the ADC measurement. The size of ROI was ≥15 mm^2 and the area ranged from 30 to 100 mm^2. Three ROIs within the area were used for kinetic analysis. Obvious cystic areas were avoided for ROIs, which was for time-signal intensity curve construction and ADC measurement. The lowest ADC of three ROIs was selected.

Immunohistochemical analyses for microvessel density (MVD) and Ki67

Formalin-fixed, paraffin-embedded sections of breast specimens were placed on sterile glass cover slips, penetrated by Triton X-100 for 1 h, and blocked by normal goat serum for 1 h at 37°C. Then, the slides were incubated with CD31 (Abcam, Cambridge, MA, USA; Cat#: ab28364), CD105 (Abcam; Cat#: ab107595) or Ki67 antibody (Abcam; Cat#: ab16667) overnight at 4°C and subsequently incubated with goat anti-mouse or goat anti-rabbit antibody (LI-COR/Rockland) for 1 h. The slides were washed with PBS, stained nuclei with DAPI (Roche Molecular Biochemicals) for 5 min at room temperature. Immunohistochemistry was analyzed under a fluorescence microscope (Nikon, Japan).

The MVD was evaluated by the immunohistochemical analysis of tumor vessels for CD31 and CD105 expression. An individual vessel was defined as an immune-positive single cell or a cluster of cells with clear lumen. Areas with fibrosis, necrosis, and inflammation, as well as vessels with a muscle wall, were excluded from the count. The sections were scanned at a magnification of 40× by two observers simultaneously to select the most vascularized areas (hot-spots) of the three tissue array spots for each patient. The microvessels in the hot-spots were counted at a magnification of 100× and their density was expressed as the mean number of microvessels/mm^2. Mean values of CD31 and CD105 staining were calculated for each individual tumor.

Ki67 expression was assessed with Image Pro Plus 6.0. Five areas were analyzed in each immunostaining slide and each area was divided into 100 squares. The percentage of Ki67-positive staining was classified into weakly positive (+ for 10–25%), positive (++ for 25–50%) and strong positive (+++ for >50%). Results are shown as the percentage of area occupied by Ki67 positive staining over the total area examined.

Statistical analysis

All data are presented as mean ±SEM. The chi-square test was used to analyze significance between malignant and benign lesions. One-way analysis of variance (ANOVA) followed by Dunnett's test was used for multiple group comparisons. Pearson analysis was used to evaluate the correlation between MRI measurements and pathological indicators. A two-tailed value of $p<0.05$ was considered as a statistically significant difference. All computations were done with SPSS 18.0.

Results

Clinical characteristics of breast lesions

Breast lesions were classified as malignant lesions in 59/124 patients (including invasive ductal carcinoma (IDC), invasive lobular carcinoma, ductal carcinoma *in situ* (DCIS), medullary carcinoma, and mucinous carcinoma) and benign lesions in 65/124 patients (including fibrocystic breast disease, fibroadenoma, intraductal papilloma, and mammary ductal dysplasia MDD). Clinical manifestations included breast lumps, breast tingling, inverted nipple, and nipple discharge. Table 1 shows the histopathological characterizations of varying types of lesions.

Characteristics of MRI in patients with breast cancer

The DCE-MRI measurements are presented in Table 2. MRI demonstrated that benign lesions were characterized primarily by morphological alterations: round or oval-based shape with clear and sharp boundaries. However, mastitis, mammary ductal hyperplasia, and atypical form of adenovirus had irregular shapes with rough fuzzy boundaries. The dynamic contrast-enhanced features revealed by DCE-MRI showed that benign breast lesions mostly had no enhancement or had early low-ratio, homogeneous enhancement and progressive TIC. In contrast, malignant breast lesions had multiple patterns, such as lobulated, round, or irregular shape, and common glitches or spines surrounded by rough blurred "crab feet"-like edges. Most of the malignant lesions had heterogeneous enhancement or annular enhancement with DCE-MRI. In addition, apparent early enhancement was observed, and TIC was mainly of multi-platform and dissection types.

Indexed in: [Current Contents/Clinical Medicine] [SCI Expanded] [ISI Alerting System] [ISI Journals Master List] [Index Medicus/MEDLINE] [EMBASE/Excerpta Medica] [Chemical Abstracts/CAS] [Index Copernicus]

Table 1. Histopathological characteristics of benign and malignant breast lesions.

Tumor group	Number	Percentage
Malignant lesions	**59**	**47.58**
Invasive ductal carcinoma	14	11.29
Invasive lobular carcinoma	35	28.23
Ductal carcinoma *in situ*	7	5.65
Medullary carcinoma	2	1.61
Mucinous carcinoma	1	0.81
Benign lesions	**65**	**52.42**
Adenosis	24	19.35
Fibroadenoma	20	16.13
Intraductal papilloma	5	4.03
Mammary ductal dysplasia	9	7.26
Inflammation	7	5.65

The data from MIP (maximum intensity projection) showed that benign breast lesions had no or only one blood vessel, whereas malignant lesions had two or more blood vessels. There was visible local skin thickening and sagging, and occasionally orange peel-like skin change when malignant lesions occurred superficially in the skin and Cooper's ligament. Nipple retraction or bridge levy was observed when tumors invaded into the nipple and milk ducts. The fat line between pathological lesions and muscle disappeared if the lesions were located deep into the pectoral muscle and fascia. In addition, 11/59 malignant lesions had axillary lymph node metastasis, 7/59 demonstrated lateral skin thickening, and 5/59 developed nipple and skin sagging.

By comparison, among the benign breast lesions, 27 had lobulated and irregular forms of nidus; 20 had annular or irregular enhancement; 17 had early high-ratio enhancement with a platform or clearance type of TIC; and seven had more than two blood vessels. Three DCIS cases were misdiagnosed as breast adenosis, which had irregular flake-like shapes and even enhancement with progressive TIC and without blood vessels, but did not have any defined lump. Another four IDC were misdiagnosed as fibro adenomas, which were rounded in shape with distinct contour, even enhancement, and a platform type of TIC with only one blood vessel.

Comparisons of MRI parameters among normal glands, benign lesions, and malignant lesions

As shown in Table 3, mean value of K^{trans} in the malignant lesion group was significantly higher than that of the benign lesion and normal gland groups ($p<0.001$), despite (in rare cases) the values overlapping between benign lesions and malignant lesions. On the other hand, K^{trans} in the benign lesion group was higher than the normal gland group (0.280±0.193 *vs.* 0.049±0.021,

Table 2. DCE-MRI Performance of benign and malignant breast lesions.

	DCE-MRI performance	Malignant lesions n=59		Benign lesions n=65		χ^2	*p* value
Shape	Regular	13	(22.03)	38	(58.46)	16.95	<0.01
	Irrrgular	46	(77.97)	27	(41.54)		
Edge	Clear	13	(22.03)	41	(63.08)	21.19	<0.01
	Rough fuzzy	46	(77.97)	24	(36.92)		
Enhanced Features	Homogeneous or no enhancement	7	(11.86)	45	(69.23)	42.39	<0.01
	Heterogeneous enhancement	28	(47.46)	13	(20.00)		
	Ring enhancement	24	(40.68)	7	(10.77)		
TIC	subtype I	1	(1.69)	50	(76.92)	78.33	<0.01
	subtype II	21	(35.59)	12	(18.46)		
	subtype III	37	(62.71)	3	(4.62)		
MIP	0	2	(3.39)	51	(78.46)	81.15	<0.01
	1	2	(3.39)	7	(10.77)		
	≥2	55	(93.22)	7	(10.77)		

Indexed in: [Current Contents/Clinical Medicine] [SCI Expanded] [ISI Alerting System] [ISI Journals Master List] [Index Medicus/MEDLINE] [EMBASE/Excerpta Medica] [Chemical Abstracts/CAS] [Index Copernicus]

Table 3. DCE-MRI parameters of normal glands, benign lesions and malignant lesions.

DCE-MRI Parameters	Normal n=59	Benign n=65	Malignant n=59	*p* value benign *vs.* normal	*p* value malignant *vs.* normal	*p* value malignant *vs.* benign
K^{trans} (min^{-1})	0.049±0.021	0.280±0.193	0.783±0.209	<0.001	<0.001	<0.001
K_{ep} (min^{-1})	0.121±0.079	0.483±0.259	1.304±0.335	<0.001	<0.001	<0.001
V_e	0.523±0.225	0.633±0.293	0.620±0.160	0.020	0.008	0.760

Table 4. DCE-MRI parameters of mammary ductal dysplasia, ductal carcinoma *in situ* and invasive ductal carcinoma.

DCE-MRI Parameters	Ductal dysplasia n=9	Ductal carcinoma *in situ* n=14	Invasive ductal carcinoma n=41	*p* value DCIS *vs.* MDD	*p* value IDC *vs.* MDD
K^{trans} (min^{-1})	0.313±0.238	0.713±0.169	0.803±0.224	<0.001	<0.001
K_{ep} (min^{-1})	0.449±0.296	1.282±0.375	1.338±0.326	<0.001	<0.001
V_e	0.729±0.318	0.601±0.172	0.617±0.159	0.292	0.329
ADC	1.221±0.113	1.008±0.097	0.947±0.236	<0.001	<0.001

p<0.001). Similarly, the averaged K_{ep} was significantly greater in malignant lesions than in benign lesions and normal glands (*p*<0.001), and greater in benign lesions relative to normal glands (0.483±0.259 *vs.* 0.121±0.079, *p*<0.001). V_e values were slightly lower in malignant lesions than in benign lesions (0.620±0.160 *vs.* 0.633±0.293, *p*=0.760), but significantly higher than in normal glands (*p*=0.008). V_e in benign lesions was also significantly greater compared with normal glands (*p*=0.020).

MRI parameters in MDD, IDC, and DCIS

DCE-MRI parameters were further compared among MDD, IDC, and DCIS. As shown in Table 4, K^{trans} and K_{ep} values were significantly higher in IDC and DCIS than in MDD. In sharp contrast, ADC values were lower in IDC and DCIS than in MDD. V_e was not significantly different among the three groups; for instance, the averaged K^{trans} value was 0.713±0.169/min DCIS and 0.803±0.224 for IDC, whereas it was 0.313±0.238 for MDD. The averaged K_{ep} value was 1.282±0.375 and 1.338±0.326 in DCIS and IDC, respectively, and was 0.449±0.296 in MDD.

Correlation between MRI parameters and pathological indicators

To further explore the association between MRI parameters and pathological indicators in malignant breast cancer, we examined the status of angiogenesis and proliferation in breast cancer by applying immunohistochemistry to assess the expression of CD31, CD105, and Ki67 in breast cancer samples. We found that the expression of CD31, CD105, and Ki67 was significantly increased in patients with DCIS and IDC compared with those with MDD (Figure 1), indicating that there were more neovascularization and proliferative cells in DCIS and IDC than in MDD. The data from DCE-MRI showed that K^{trans} and K_{ep} were markedly higher in DCIS and IDC than in MDD, whereas the ADC value showed the opposite alterations (Table 4). Table 5 shows that the mean K^{trans} or K_{ep} values were positively correlated with CD105 level (*p*=0.024, r=0.563, or *p*=0.010, r=0.723, respectively). The mean ADC value showed a significant inverse correlation with Ki67 (*p*=0.025, r=-0.566).

Discussion

Breast cancer is the most common malignancy in women, and the incidence is still increasing [11]. There is an urgent need for early diagnosis of breast cancer. However, due to the complex pathological processes, it is difficult to diagnose breast cancer at an early stage [12]. In recent years, MRI has been developed as a highly sensitive and specific tool for breast cancer diagnosis [13]. In the present study, we evaluated the value of conventional morphological examination in conjunction with DCE-MRI for more precise diagnosis of breast cancer. We found that CD105 and Ki67, the commonly recognized markers for angiogenesis and proliferation, respectively, were closely correlated with MRI parameters. These results provide further evidence for the feasibility and accuracy of MRI in diagnosis of breast cancer. Moreover, our findings suggest that determination of K^{trans}, $K_{ep,}$ and ADC values permits estimation of tumor angiogenesis and proliferation in breast cancer, and DCE-MRI parameters can be used as imaging biomarkers to predict the biologic aggressiveness of the tumor and patient prognosis.

Indexed in: [Current Contents/Clinical Medicine] [SCI Expanded] [ISI Alerting System] [ISI Journals Master List] [Index Medicus/MEDLINE] [EMBASE/Excerpta Medica] [Chemical Abstracts/CAS] [Index Copernicus]

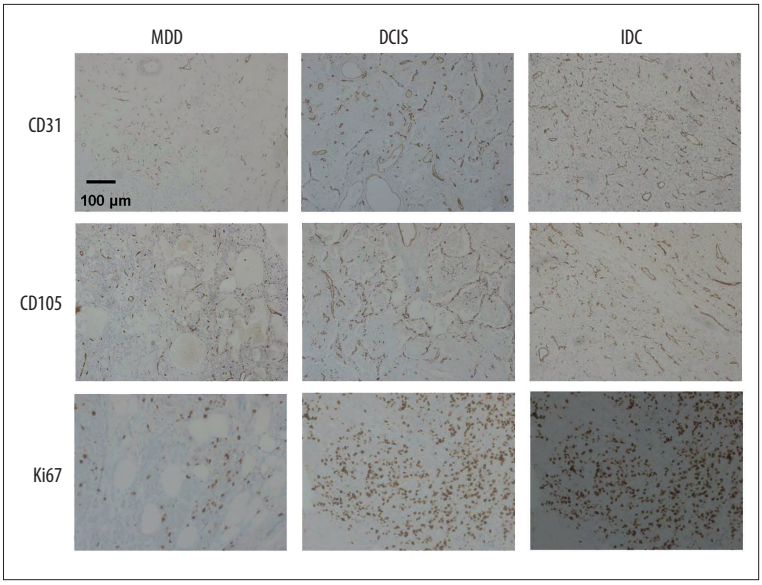

Figure 1. Comparison of expression of CD31, CD105, and Ki67 in the patients with MDD, DCIS and IDC, as assessed by immunohistochemistry.

Table 5. Correlation between DCE-MRI parameters and pathological indicators.

	CD31		CD105		Ki67	
	r value	*p* value	r value	*p* value	r value	*p* value
K^{trans} (min^{-1})	0.187	0.393	0.563	0.024	0.329	0.092
K_{ep} (min^{-1})	0.295	0.164	0.723	0.010	0.418	0.061
V_e	–0.105	0.635	–0.075	0.888	–0.540	0.268
ADC	–0.079	0.721	–0.293	0.271	–0.566	0.025

Positive correlation between CD105 and K^{trans} or K_{ep}

Compared to normal tissues, tumors require more rigorous supplies of nutrients and oxygen, as well as an enhanced capacity to eliminate metabolic wastes and carbon dioxide [14]. In meeting these needs, tumors develop a more active process of angiogenesis to promote the tumor-associated neovasculature. Indeed, angiogenesis is not only a basis for solid tumor growth and metastasis, but is also an important determinant for prognosis [15,16]. Recent studies found that MVD is closely related to metastasis and tumor recurrence [17,18]. Although a number of molecules expressed in vascular endothelial cells, including CD31, CD34, and FVIII, have been used as essential markers for angiogenesis, their instability in proliferative microvascular cells of tumor tissues has hampered their applications. Thus, whether MVD count can be used to determine the prognosis of malignant tumors remains controversial. In contrast, CD105, belonging to the transformation growth factor-β (TGF-β) family, is highly expressed in endothelial cells of tumor vessels, but only minimally expressed in normal vessels [19,20]. Zhang et al. identified CD105 as a marker of endothelial cells involved in the process of tumor angiogenesis [21]. CD105 was found to be inversely proportional to the survival of cancer patients [22]. These findings suggest CD105 as a novel indicator for predicting cancer development and prognosis.

In this study, we found that the expression of CD31 and CD105 in breast cancer was significantly higher than that in normal breast tissue. These results indicate that there is increased neovascularization in breast cancer, which may play a key role in supplying nutrition for the development and metastasis of breast cancer. Moreover, our results showed that MRI parameters K^{trans} and K_{ep} values were significantly higher in malignant than in benign lesions. Furthermore, CD105, but not CD31, was closely correlated with MRI parameters K^{trans} or K_{ep} values, indicating that K^{trans} and/or K_{ep} in combination with CD105 might serve as a better diagnostic marker for breast cancer.

Ki67 in combination with MRI parameters for early diagnosis of breast cancer

In contrast to K^{trans} and K_{ep} values, ADC values were significantly lower in malignant than in benign lesions, and the mean ADC values were inversely correlated with Ki67. These results indicate that in addition to K^{trans} and K_{ep} values, ADC might also offer a valuable MRI parameter for breast cancer

Indexed in: [Current Contents/Clinical Medicine] [SCI Expanded] [ISI Alerting System] [ISI Journals Master List] [Index Medicus/MEDLINE] [EMBASE/Excerpta Medica] [Chemical Abstracts/CAS] [Index Copernicus]

diagnosis, particularly when combined with the histological parameter Ki67.

Sustained proliferation is a hallmark of cancer [14]. Ki67, a nuclear antigen expressed in the nucleus of cells in active proliferation, is considered a valid nuclear marker of cell proliferation. Studies have shown that expression of Ki67 is upregulated in a variety of human tumors, such as breast cancer, cervical cancer, non-Hodgkin's malignant tumor, and glioma [10,23]. Evidence also exists showing that increased expression of Ki67 reflects proliferation of malignant tumor cells in breast cancer, lung cancer, colorectal cancer, and other cancers [24]. The positive staining of Ki67 also provided evidence for the use of Ki67 in combination with MRI for early diagnosis of breast cancer.

Conclusions

We have demonstrated that MRI parameters K^{trans}, $K_{ep,}$ and ADC allow an estimation of tumor angiogenesis and proliferation in breast cancer and, when combined with the histological features such as CD105 or Ki67, these parameters can be used as imaging biomarkers for more precise and earlier prediction of the biologic aggressiveness and prognosis of breast tumors.

Conflict of interest

The authors state no conflict of interest.

References:

1. Peters NH, Borel Rinkes IH, Zuithoff NP et al: Meta-analysis of MR imaging in the diagnosis of breast lesions. Radiology, 2008; 246: 116–24
2. Huang W, Fisher PR, Dulaimy K et al: Detection of breast malignancy: diagnostic MR protocol for improved specificity. Radiology, 2004; 232: 585–91
3. Dmuchowska DA, Krasnicki P, Obuchowska I et al: Ophthalmic manifestation of skull base metastasis from breast cancer. Med Sci Monit, 2012; 18(11): CS105–8
4. Bluemke DA, Gatsonis CA, Chen MH et al: Magnetic resonance imaging of the breast prior to biopsy. JAMA, 2004; 292: 2735–42
5. Nunes LW, Schnall MD, Orel SG: Update of breast MR imaging architectural interpretation model. Radiology, 2001; 219: 484–94
6. Fitzgibbons PL, Page DL, Weaver D et al: Prognostic factors in breast cancer. College of American Pathologists Consensus Statement 1999. Arch Pathol Lab Med, 2000; 124: 966–78
7. Charpin-Taranger C, Dales JP, Garcia S et al: [The immunohistochemical expression of CD105 is a marker for high metastatic risk and worse prognosis in breast cancers]. Bull Acad Natl Med, 2003; 187: 1129–45; discussion 1145–46 [in French]
8. Wang JM, Kumar S, Pye D et al: A monoclonal antibody detects heterogeneity in vascular endothelium of tumours and normal tissues. Int J Cancer, 1993; 54: 363–70
9. Yasukawa T, Kimura H, Tabata Y et al: Active drug targeting with immunoconjugates to choroidal neovascularization. Curr Eye Res, 2000; 21: 952–61
10. Sun JZ, Chen C, Jiang G et al: Quantum dot-based immunofluorescent imaging of Ki67 and identification of prognostic value in HER2-positive (non-luminal) breast cancer. Int J Nanomedicine, 2014; 9: 1339–46
11. Khanna S, Dash PR, Darbre PD: Exposure to parabens at the concentration of maximal proliferative response increases migratory and invasive activity of human breast cancer cells *in vitro*. J Appl Toxicol, 2014; 34(9): 1051–59
12. Giess CS, Raza S, Birdwell RL: Distinguishing breast skin lesions from superficial breast parenchymal lesions: diagnostic criteria, imaging characteristics, and pitfalls. Radiographics, 2011; 31: 1959–72
13. Faermann R, Sperber F, Schneebaum S et al: Tumor-to-breast volume ratio as measured on MRI: a possible predictor of breast-conserving surgery versus mastectomy. Isr Med Assoc J, 2014; 16: 101–5
14. Hanahan D, Weinberg RA: Hallmarks of cancer: the next generation. Cell, 2011; 144: 646–74
15. Wang Y, Ma W, Zheng W: Deguelin, a novel anti-tumorigenic agent targeting apoptosis, cell cycle arrest and anti-angiogenesis for cancer chemoprevention. Mol Clin Oncol, 2013; 1: 215–19
16. Crew KD, Ho KA, Brown P et al: Effects of a green tea extract, Polyphenon E, on systemic biomarkers of growth factor signalling in women with hormone receptor-negative breast cancer. J Hum Nutr Diet, 2104 [Epub ahead of print]
17. Yang T, Chen M, Sun T: Simvastatin attenuates TGF-beta1-induced epithelial-mesenchymal transition in human alveolar epithelial cells. Cell Physiol Biochem, 2013; 31: 863–74
18. Wang WQ, Liu L, Sun HC et al: Tanshinone IIA inhibits metastasis after palliative resection of hepatocellular carcinoma and prolongs survival in part via vascular normalization. J Hematol Oncol, 2012; 5: 69
19. Paschoal JP, Bernardo V, Canedo NH et al: Microvascular density of regenerative nodule to small hepatocellular carcinoma by automated analysis using CD105 and CD34 immunoexpression. BMC Cancer, 2014; 14: 72
20. Grigore D, Simionescu CE, Stepan A et al: Assessment of CD105, alpha-SMA and VEGF expression in gastric carcinomas. Rom J Morphol Embryol, 2013; 54: 701–7
21. Zhang Y, Hong H, Nayak TR et al: Imaging tumor angiogenesis in breast cancer experimental lung metastasis with positron emission tomography, near-infrared fluorescence, and bioluminescence. Angiogenesis, 2013; 16: 663–74
22. Cao JJ, Zhao XM, Wang DL et al: YAP is overexpressed in clear cell renal cell carcinoma and its knockdown reduces cell proliferation and induces cell cycle arrest and apoptosis. Oncol Rep, 2014; 32: 1594–600
23. Sari Aslani F, Safaei A, Pourjabali M et al: Evaluation of Ki67, p16 and CK17 Markers in Differentiating Cervical Intraepithelial Neoplasia and Benign Lesions. Iran J Med Sci, 2013; 38: 15–21
24. Kontzoglou K, Palla V, Karaolanis G et al: Correlation between Ki67 and breast cancer prognosis. Oncology, 2013; 84: 219–25

Indexed in: [Current Contents/Clinical Medicine] [SCI Expanded] [ISI Alerting System] [ISI Journals Master List] [Index Medicus/MEDLINE] [EMBASE/Excerpta Medica] [Chemical Abstracts/CAS] [Index Copernicus]